A Study of a Variable Sonic Ejector Flow

Jun-Hee Lee and Heuy-Dong Kim
Andong National University
School of Mechanical Engineering, 388 Songchun-Dong, Andong, 760-749, Korea
kimhd@andong.ac.kr

Keywords: Compressible Flow, Sonic Ejector, Hydrogen Fuel Cell, Entrainment Ratio, Throat Area Ratio

Abstract

A cone cylinder is used to obtain variable operation conditions for the sonic ejector-diffuser system. The cone cylinder is designed to be shifted upstream and downstream to change the ejector throat area ratio, thus obtaining variable mass flow rates. The present study investigates the effects of ejector throat area ratio and operating pressure ratio on the entrainment of secondary stream for the variable sonic ejector system. The study is carried out experimentally. The ejector throat area is varied at the range from ψ=11.88 to 66.69, and the operating pressure ratio is changed from p_{0p}/p_a=1.25 to 9.0. The results show that the variable sonic ejector system can be operated to obtain specific entrainment ratio of secondary stream by altering the ejector throat area ratio and operating pressure ratio.

Introduction

Ejector system is a device to transport a low-pressure secondary flow by using a high-pressure primary flow. Ejector system is, in general, composed of primary nozzle, mixing section, and diffuser[1], and it can induce the secondary flow or affect the secondary chamber pressure condition by both shear stress and pressure drop which are generated in the primary jet boundary. Ejector system is simple in construction and has no moving parts, so it can not only compress and transport a massive capacity of fluid without trouble, but also has little need for maintenance. Currently, ejector system is utilized for the thrust augmentation of V/STOL aircraft[2,3], high-altitude state simulation facility[4], combustion facility[5], refrigeration/air conditioning[6], ventilation/deodorization[7], noise-control device[8], etc., and it is recently applied to a equipment for reducing the amount of hydrogen consumption in a hydrogen fuel cell.

Hydrogen fuel cell generates electricity by the reverse process of the electrolysis of pure water into hydrogen and oxygen. In hydrogen fuel cell, the ejector system recirculate the some amount of hydrogen consumed for electrode reaction and thus can economize hydrogen consumption. Hydrogen fuel cell is prospected to substitute the petroleum based fuel which is confronted with the air pollution and exhaustion, and to be applied for an automobile as a power source in the future. However, the mileage of the automobile with hydrogen fuel cell is quite short due to the limited volume and pressure of the hydrogen fuel tank.

Hydrogen consumption affects the output of power of an automobile with hydrogen fuel cell. After electrode reaction, the amount of collected hydrogen should be controlled depend upon the output of power. In the case of adopting conventional ejector system for hydrogen fuel cell, it can only recirculate constant rate of hydrogen independent of the output of power of an automobile, because the shape of the components like driving nozzle and diffuser are fixed. Therefore the conventional ejector system is not fit to the hydrogen fuel cell.

Up to date, few works on the ejector system which can control the amount of recirculation rate of hydrogen depending on the fuel cell load have been performed throughout the world, and its development is indispensable for the next generation hydrogen fuel cell vehicle.

The present experimental study investigates the flow characteristics of a variable ejector system which can adjust the hydrogen recirculation rate depending on the output of power of fuel cell. A sonic nozzle is adopted as a primary nozzle, and a cone-type cylinder which can shift upstream and downstream is equipped in the flow axis for altering the sectional area at the primary nozzle exit. In order to examine the effects of the ejector throat area ratio on the secondary flow rate and the ejector flow field, the ejector throat area ratio is varied at the range from ψ=11.88 to 66.69, and the operating pressure ratio is changed from p_{0p}/p_a=1.25 to 9.0.

Experimental Apparatus

Variable Sonic Ejector

Fig. 1 and Table 1 represent the detailed shapes and dimensions of the variable sonic ejector adopted in this study. All the configurations are fixed except the cylinder. The cone-type cylinder can shift upstream and downstream to change the sectional area at the nozzle exit(A_n), thereby to vary the ejector throat area ratio(ψ). In the present study, the ejector throat area

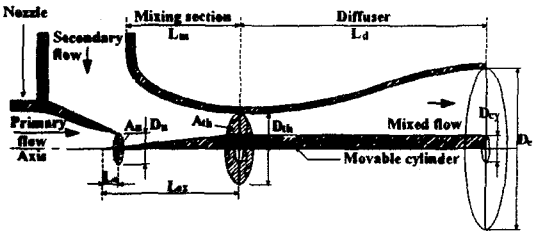

Fig. 1 Schematics of variable sonic ejector

Table 1 Variable sonic ejector geometric parameters

ψ	A_n (mm^2)	A_{th} (mm^2)	L_o (mm)
11.88	27.77	329.867	2.7
12.68	26.00	329.867	8.32
13.78	23.94	329.867	14.34
15.73	20.97	329.867	20.48
18.83	17.52	329.867	26.34
25.93	12.72	329.867	32.54
46.88	7.04	329.867	38.56
66.69	4.95	329.867	40.58

D_n (mm)	6	L_m (mm)	55	L_o (mm)
D_{th} (mm)	22	L_d (mm)	115	
D_{cy} (mm)	8	L_{ex} (mm)	59.7	
D_e (mm)	54			

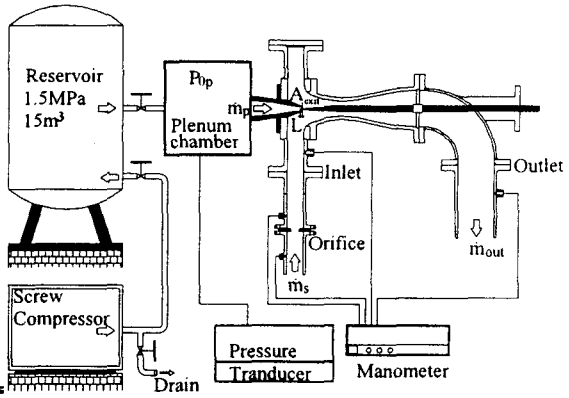

Fig. 2 Schematics of experimental apparatus

Experimental setup and procedures

Fig. 2 shows the schematic diagram of the experimental setup for the present study. The apparatus consists of compressor, reservoir, primary plenum chamber, variable sonic ejector and measuring system. The compressed air at 1.5MPa in the reservoir is induced to the primary plenum chamber, where the flow is restored to its stagnation conditions, and discharged into the ejector mixing section through the sonic nozzle. The discharged jets entrain the secondary flow by shear stress, and the primary jets and entrained secondary flow are mixed in the mixing section and discharged into the atmosphere through the ejector diffuser. At this moment, the cone-type cylinder shifts upstream and downstream at the range ψ=11.88~66.69, and the operating pressure ratio varies p_{0p}/p_a=1.25~9.0.

The mass flow rate of the primary stream can be calculated from pressure at the plenum chamber[9], and the secondary stream mass flow rate is measured from the orifice installed in the secondary stream inlet[10]. If the pressures at the orifice upstream(p_1) and downstream(p_2), the densities at the orifice upstream(ρ_1) and downstream(ρ_2), and areas of at the orifice entrance(A_1) and plate(A_2) are given, the secondary stream mass flow rate is obtained from the following equation.

$$\dot{m}_s = \rho_2 A_2 \left[\frac{\frac{2\gamma}{\gamma-1}\frac{p_1}{\rho_1}\left\{1-\left(\frac{p_2}{p_1}\right)^{\frac{\gamma-1}{\gamma}}\right\}}{1-\left(\frac{p_2}{p_1}\right)^{\frac{2}{\gamma}}\left(\frac{A_2}{A_1}\right)^2} \right]^{\frac{1}{2}} \quad (1)$$

To validate the above equation, the coefficient of discharge is obtained letting the secondary stream mass flow rate equal to the primary stream mass flow rate blocking off the outlet.

In the present experiment, wall pressures at the inlet, outlet, and at the orifice upstream and downstream are measured using the mercury manometer.

Experimental Results and Discussions

Fig. 3 shows the effect of operating pressure ratio on the secondary flow entrainment ratio when the ejector throat area ratio is a parameter. The secondary flow entrainment ratio is defined as the ratio of the secondary mass flow rate and the output mass flow rate. For each constant ψ, the secondary flow entrainment ratio decreases as the operating pressure ratio increases accompanying with small fluctuation at the range of p_{0p}/p_a=1.75~4.0. When ψ=11.88, the fluctuation occurs around p_{0p}/p_a=4.0, and others at the range of p_{0p}/p_a=1.75~3.0. The rise of the secondary flow entrainment ratio around p_{0p}/p_a=2.0 seems that

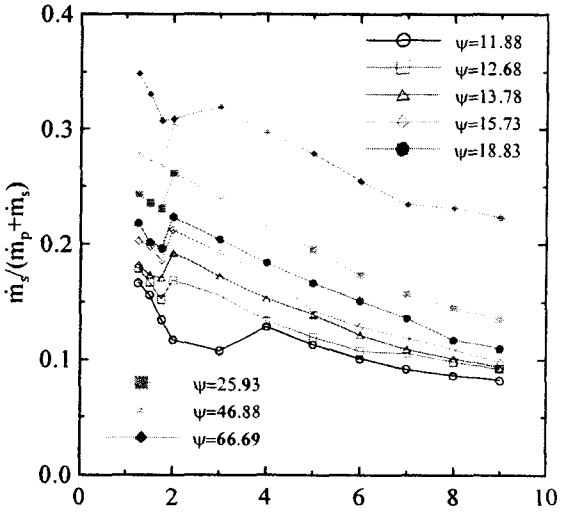

Fig. 3 Relationship between $m_s/(m_p+m_s)$ and p_{0p}/p_a

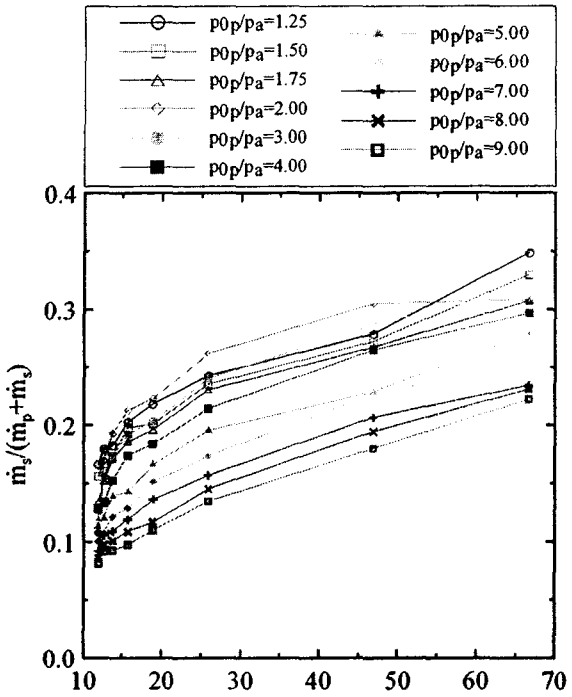

Fig. 4 Relationship between $m_s/(m_p+m_s)$ and ψ

the overexpanded flow generates series of shocks in the mixing section and makes the flow unstable.

Fig. 4 shows the secondary flow entrainment ratio when the ejector throat area ratio changes. For a constant operating pressure ratio, the secondary flow entrainment ratio increases in accordance with the increment of ψ. When ψ is less than ψ=20, the increment shows sudden change. However, the rate of increment of the secondary flow entrainment becomes lax. Moreover, when ψ is low, the secondary flow entrainment ratio distribution is gathered, but it becomes scattered as ψ is increasing.

From the results of Fig. 3 and Fig. 4, it is possible to locate the secondary flow entrainment ratio on any position by adjusting the ejector throat area ratio and the operating pressure ratio.

Fig. 5 shows the secondary mass flow rate variations with the operating pressure ratio when the ejector throat area ratio is a parameter. The secondary mass flow rate increases as the operating pressure ratio increases. For a specific operating pressure ratio, the secondary mass flow rate distributes narrowly when the operating pressure ratio is low, but as the operating pressure ratio increases, the secondary mass flow rate distributions become large. This means that the secondary mass flow rate is highly affected by the ejector throat area ratio when the operating pressure ratio is large.

Fig. 6 shows the secondary mass flow rate variations with the ejector throat area ratio when the operating pressure ratio is a parameter. There is a sudden increment of the secondary mass flow rate at the range of ψ=11.88~1.78, and the secondary mass flow rate becomes decrease as the ejector throat area

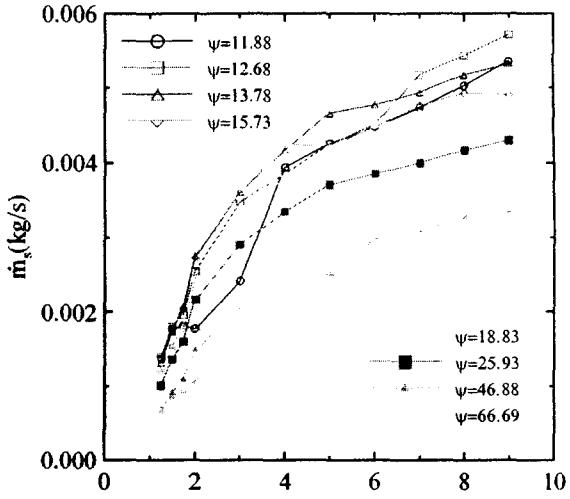

Fig. 5 Secondary mass flow rate variations vs. p_{0p}/p_a

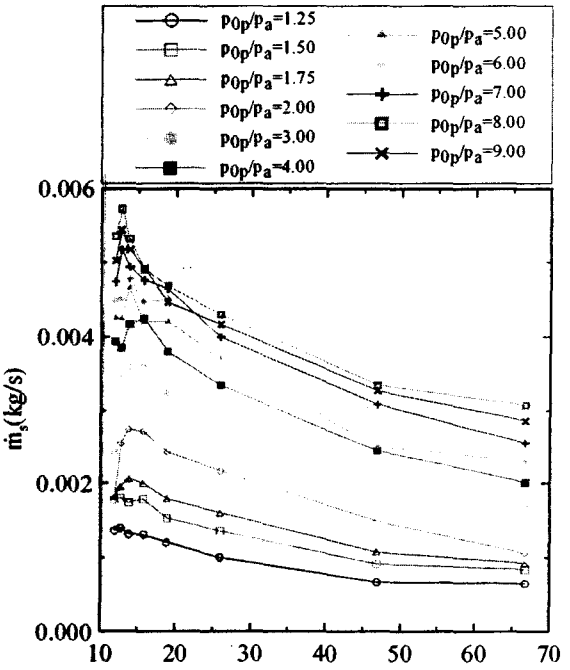

Fig. 6 Secondary mass flow rate variations vs. ψ

ratio is increasing. For a specific ejector throat area ratio, the secondary mass flow rate distributions become narrow as the ejector throat area ratio is increasing, and vice versa. It also verifies that the secondary mass flow rate variation is sensitive to the operating pressure ratio when the ejector throat area ratio is small.

Fig. 7 shows the effects of the ejector throat area ratio on the inlet wall pressure variations. In the ordinates, the wall pressure at the secondary flow inlet is normalized with the ambient pressure. From the figure, the inlet wall pressures distribute loosely when the ejector throat area ratio is low, but it become converged when the ejector throat area ratio increases.

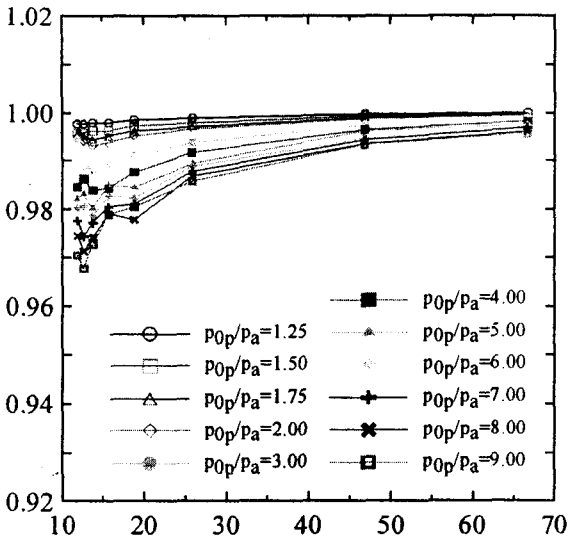

Fig. 7 Inlet wall pressure variations vs. ψ

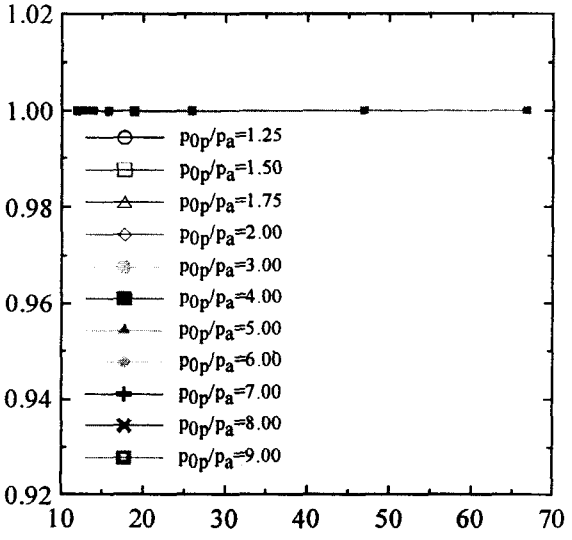

Fig. 8 Outlet wall pressure variations vs. ψ

It shows that the wall pressure at the secondary flow inlet is sensitive to the operating pressure ratio when the ejector throat area ratio is low.

Fig. 8 shows the wall pressure distributions at the outlet for various ejector throat area ratios and operating pressure ratios. In the ordinates, the wall pressure at the outlet is normalized with the ambient pressure. It shows that the wall pressure at the outlet is almost equal to the ambient pressure for all ranges of p_{0p}/p_a and ψ.

Conclusion

The present study investigated effects of ejector throat area ratio and operating pressure ratio on the secondary flow entrainment ratio of the variable sonic ejector for the purpose of applying it to the hydrogen fuel cell for vehicle. The results are summarized as follows.

(1) The variable sonic ejector system can be operated to obtain specific entrainment ratio of secondary stream by altering the ejector throat area ratio and operating pressure ratio.

(2) The secondary mass flow rate is getting highly affected by the ejector throat area ratio as the operating pressure ratio becomes increasing.

(3) The wall pressure at the outlet is non-sensitive to the operating pressure ratio and ejector throat area ratio.

References

1) Keenan, J. H., Neumann, E. P., and Lustwerk, F.: An Investigation of Ejector Design by Analysis and Experiment, *Journal of Applied Mechanics*, 17 (3), 1950, pp. 299-309.

2) Alperin, M. and Wu, J. J.: Thrust Augmenting Ejector, Part 2, *AIAA Journal*, 21 (12), 1983, pp. 1698-1706.

3) Yang, T. T., Ntone, F., Jiang, T., and Pitts, D. R.: An Investigation of High Performance, Short Thrust Augmenting Ejectors, *Journal of Fluids Engineering*, 107, 1985, pp. 23-30.

4) Quinn, B.: Ejector Performance at High Temperatures and Pressures, *Journal of Aircraft*, 13 (12), 1976, pp. 948-954.

5) Francis, W. E., Hoggarth, M. L., and Templeman, J. J.: The Design of Jet Pumps and Injectors for Gas Distribution and Combustion Purposes, The Symposium on Jet Pumps and Ejectors, BHRA Fluid Engineering-Institution of Chemical Engineers, London, England, No. 6, 1972, pp. 81-96.

6) Hsu, C. T.: Investigation of an Ejector Heat Pump by Analytical Methods, ORNL/CON-144, Oak Ridge National Laboratory, July, 1984.

7) Knight, J.: The Use of Steam Ejector for the Vacuum Degassing of Steel, *Journal of IMech*, 181 (10), 1967, pp. 225-239.

8) Viets, H., Campbell, J. R., and Korkan, K. D.: Acoustic Interactions in Ejectors, AIAA Paper 81-2045, Oct., 1981.

9) Oosthuizen, P. H. and Carscallen, W. E.: *Compressible Fluid Flow*, McGraw-Hill Book Co., 1997, pp. 192-195.

10) Kim, H. D.: Effect of Boundary Layer Suction on Shock Wave/Boundary Layer Interaction, Proceedings of the KSME 1996 Fall Annual Meeting B, 1996, pp. 274-280.